Spectrochimica Acta Part A: Molecular and Biomolecular Spectroscopy 192 (2018) 263–274

Contents lists available at ScienceDirect

Spectrochimica Acta Part A: Molecular and Biomolecular Spectroscopy

journal homepage: www.elsevier.com/locate/saa

Synthesis, spectroscopic and TD-DFT quantum mechanical study of azo-azomethine dyes. A laser induced *trans-cis-trans* photoisomerization cycle

Anton Georgiev [a,*], Anton Kostadinov [a], Deyan Ivanov [b], Deyan Dimov [b], Simeon Stoyanov [c], Lian Nedelchev [b], Dimana Nazarova [b], Denitsa Yancheva [c]

[a] Department of Organic Chemistry, 1756 Sofia, 8 St. Kliment Ohridski Blvd, University of Chemical Technology and Metallurgy, Bulgaria
[b] Department of Optical Metrology and Holography, Department of Optical Materials, 1113 Sofia, 109 "Acad. G. Bonchev" Blvd., Institute of Optical Materials and Technologies, Bulgarian Academy of Science, Bulgaria
[c] Laboratory of Structural Organic Analysis, Sofia 1113, 9 Acad. G. Bonchev Blvd., Institute of Organic Chemistry with Centre of Phytochemistry, Bulgarian Academy of Science, Bulgaria

ARTICLE INFO

Article history:
Received 4 July 2017
Received in revised form 21 October 2017
Accepted 6 November 2017
Available online 07 November 2017

Keywords:
Azo-azomethine dyes
Schiff bases
Azobenzene dyes
DFT quantum chemical calculations
trans-cis-trans photoisomerization
Solvatochromism
Photochromism

ABSTRACT

This paper describes the synthesis, spectroscopic characterization and quantum mechanical calculations of three azo-azomethine dyes. The dyes were synthesized via condensation reaction between 4-(dimethylamino)benzaldehyde and three different 4-aminobenzene azo dyes. Quantum chemical calculations on the optimized molecular geometry and electron densities of the *trans (E)* and *cis (Z)* isomers and their vibrational frequencies have been computed by using DFT/B3LYP density-functional theory with 6-311++G(d,p) basis set in vacuo. The thermodynamic parameters such as total electronic energy *E (RB3LYP)*, enthalpy H_{298} (sum of electronic and thermal enthalpies), free Gibbs energy G_{298} (sum of electronic and thermal free Gibbs energies) and dipole moment μ were computed for *trans (E)* and *cis (Z)* isomers in order to estimate the $\Delta E_{trans \rightarrow cis}$, $\Delta\mu_{trans \rightarrow cis}$, $\Delta H_{trans \rightarrow cis}$, $\Delta G_{trans \rightarrow cis}$ and $\Delta S_{trans \rightarrow cis}$ values. After molecular geometry optimization the electronic spectra have been obtained by TD-DFT calculations at same basis set and correlated with the spectra of vapour deposited nanosized films of the dyes. The NBO analysis was performed in order to understand the intramolecular charge transfer and energy of resonance stabilization. Solvatochromism was investigated by UV-VIS spectroscopy in five different organic solvents with increasing polarity. The dynamic photoisomerization experiments have been performed in DMF by pump lasers λ = 355 nm (mostly E → Z) and λ = 491 nm (mostly Z → E) in spectral region 300 nm – 800 nm at equal concentrations and times of illumination in order to investigate the photodynamical *trans-cis-trans* properties of the —CH═N— and —N═N— chromophore groups of the dyes.

1. Introduction

The photochemistry of the azo —N═N— and azomethine —CH═N— groups has attracted much attention in recent years, because of their photodynamic properties related to the reversible *trans-cis-trans* isomerization cycle [1,2,3,4,5]. Azo-azomethine (AAM) dyes contain two photosensitive functional groups: azo —N═N— and azomethine —CH═N—, which determine their spectral and photochromic properties. The electronic absorption spectra in polar protic or aprotic solvents exhibit two absorption maxima λ_{max} ~ 365 nm for π → π* electron transitions and λ_{max} > 400 nm for n → π* electron transitions [6,7,8,9,10]. The spectral properties of AAM dyes depend on the nature of substituents in aromatic rings. Electron withdrawing (EW) and electron donating (ED) groups in *ortho* or *para* position to the chromophore groups lead to unsymmetrical electron distributions ("push-pull" effect), which decrease the electron transition energy [11,12,13,14,15]. The photoisomerization *trans-cis-trans* cycle is the main feature of both chromophore group extensively used for light driven optical switches, non-linear optical elements, reversible optical storage and other photonics applications. The *trans (E)* isomer is more thermodynamically stable than the *cis (Z)* isomer, due to the higher energy of *cis (Z)* twist conformation related to the orbitals repulsion between aromatic rings and forbidden orbital symmetry [16,17]. There are many works on photochemistry and applications of azobenzene and azomethine (Schiff base) dyes, but there is little information on photoisomerization properties of both chromophore groups in the AMM dyes [1,2,9,18,19]. The E → Z photoconversion for unsubstituted azobenzene and N-benzylideneaniline occurs upon illumination with UV light at λ = 355 nm, 10–15 nm higher in energy, where the

* Corresponding author.
E-mail address: antonchem@abv.bg (A. Georgiev).

https://doi.org/10.1016/j.saa.2017.11.016
1386-1425/

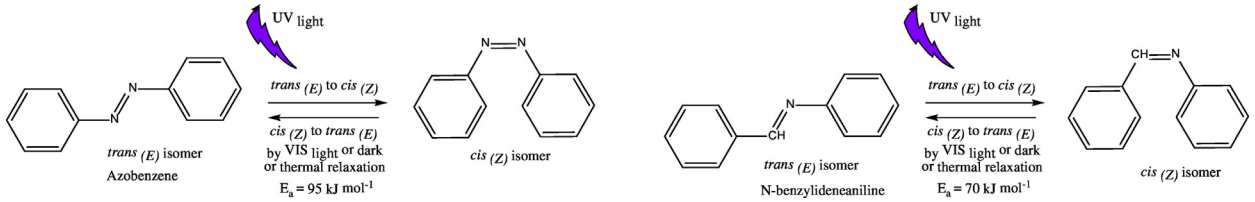

Fig. 1. Schematically illustration of *trans-cis-trans* photoisomerization of the azobenzene and N-benzylideneaniline.

chromophore groups absorb. The reversible Z → E occurs spontaneously in the dark or under VIS light or by thermal relaxation (Fig.1).

The energy of Z → E relaxation and stability of *cis (Z)* isomer mainly depend on the properties of aromatic ring substituents and the geometry of molecule. The —CH═N— group is structurally similar and is isoelectronic with —N═N— group, however aniline ring is twisted by 41–55° in regard to the plane of phenyl ring and azomethine bond is caused by the conjugation between benzene ring and nitrogen lone pair. In contrast, the azobenzene is planar. Theoretical calculations also confirm the nonplanar conformation of azomethine derivatives and planar one for azobenzenes [18,20,21]. The kinetic of the relaxation process is determined by activation energy (E_a) barrier: around 90 kJ mol^{-1} for azobenzene and 70 kJ mol^{-1} for N-benzylideneaniline, the latter value being considerably lower [18]. From practical point of view, this "double" (via azo and azomethine bonds) isomerization of AMM dyes can be applied for nanoscale molecular motors, optical storage devices and light driven photoswitches [19,22,23,24].

Many researches have studied the mechanisms of photoisomerization cycle of the aromatic azo and azomethine dyes [18,20,25,26]. Ying Luo et al. have investigated *trans-cis-trans* isomerization of several N-benzylideneaniline derivatives by theoretical calculations and experimental spectroscopy [18]. The relatively low activation energy of Z → E conversion of unsubstituted imines results in thermally unstable compounds at room temperature. However, the *ortho* and *para* substituted π-donors in the aniline ring increase considerably the relative stability of *cis (Z)* isomer. The lower activation energy barrier of the thermal Z → E isomerization of the azomethines compared to those of the azobenzenes, may be advantageous because it allows for rapid, reversible geometrical changes in light-driven molecular devices [18]. By using density-functional theory (DFT) on ground state and time-dependent DFT (TD-DFT) on excited state supported by experimental spectra, A. Gaenko et al. have been studied mechanisms of isomerization of the N-benzylideneaniline [20]. The DFT potential energy surface on θ and φ coordinates suggests that the C-N-C inversion is the preferred path for E → Z excited state and Z → E ground state isomerization [20]. It is well known that the position and nature of EW and ED lead to different isomerization pathway due to unsymmetrical electron distributions and symmetry of frontier orbitals [16,17,27,28]. Four mechanisms are proposed and proved by time resolved spectroscopy and theoretical calculations: (i) rotation; (ii) inversion; (iii) concerted inversion; (iv) inversion-assisted rotation. Multiple isomerization pathways have often been involved to explain the experimental photochemical behavior [16,17].

In our previous investigation three 4-aminoazobenzene dyes have been theoretically and spectrally characterized in order to understand their photochromic behavior [29]. In the present work we have synthesized and investigated three AAM dyes containing donor and acceptor parts. Due to the presence of two chromophore groups in the molecular backbone, the synthesized AAM dyes exhibit interesting and potentially useful physical and chemical properties. The ground state structure and electronic absorption spectra of the dyes as *trans (E)* and *cis (Z)* isomers were investigated by DFT and TD-DFT calculations in order to understand their photochromic and photodynamic properties. The experimental UV-VIS spectra of vapour deposited nanosized films and solvatochromism of the dyes were correlated with quantum mechanical calculation results. The photoinduced *trans-cis-trans* isomerization was performed by lasers illumination at λ = 355 nm (E → Z) and λ = 491 nm (Z → E).

2. Experimental

2.1. Used Materials

The starting 4-aminoazobenzenes (Azo-1, Azo-2 and Azo-3) were synthesized according to our previous work [29]. 4-(dimethylamino)benzaldehyde (98%) was purchased from Sigma Aldrich. The solvents were supplied from local supplier Valerus Ltd. and Sigma Aldrich. For the spectral investigation all solvents were spectroscopy grade purity.

2.2. General Methodology for Synthesis of the Azo-Azomethine Dyes

A solution of 2,2 mmol (0.33 g) 4-(dimethylamino)benzaldehyde, 2 mmol 4-aminoazobenzene dye and acetic acid (1 mL) in absolute ethanol (25 mL) was refluxed for 24 h. After cooling and solvent evaporation, the crude product was isolated and recrystallized two times in ethanol, after then dried in vacuum oven for 24 h. The synthesis of azo-azomethines are presented on the Scheme 1.

2.2.1. Preparation of 2-((1E)-(4-((4-(Dimethylamino)Benzylidene)Amino)-2-(Hydroxymethyl)Phenyl)Diazenyl)-5-Nitrobenzonitrile, ***AAM 1***

The AAM 1 was synthesized from 2 mmol (0.59 g) Azo-1 and 2.2 mmol (0.33 g) 4-(dimethylamino)benzaldehyde, yield 45%, m.p. 194–196 °C. ATR-FTIR cm^{-1}: 3406 and 3327 (ν —OH), 3231 (ν_{C-H} —CH═N—), 2234 (ν —C≡N), 1642 ($\nu_{C=N}$ —CH═N—), 1493 and 1317 (ν —NO_2), 1438 (ν —N═N—). ^{1}H NMR (DMSO-d_6) δ_H ppm: 3.04 (d, 6H), 3.43 (d, 2H), 4.35 (s, 1H –OH), 6.85 (d, 2H), 7.50 (d, 2H), 7.68 (d, 1H), 7.83 (d, 1H), 8.13 (dd, 2H), 8.61 (s, 1H), 9.67 (s, 1H —CH═N—). Elemental analysis calculated for $C_{23}H_{20}N_6O_3$: C, 64.48; H, 4.71; N, 19.62; O, 11.20, Found: C, 64.85; H, 4.11; N, 19.79; O, 11.76.

2.2.2. Preparation of (5-((4-(Dimethylamino)Benzylidene)Amino)-2-((E)-(2,4-Dinitrophenyl)Diazenyl)Phenyl)Methanol, ***AAM 2***

The AAM 2 was synthesized from 2 mmol (0.63 g) Azo-2 and 2.2 mmol (0.33 g) 4-(dimethylamino)benzaldehyde, yield 48%, m.p. 123–126 °C. ATR-FTIR cm^{-1}: 3446 and 3333 (ν –OH), 3195 (ν_{C-H} —CH═N—), 1625 ($\nu_{C=N}$ —CH═N—), 1522 and 1496 (ν^{as} —NO_2), 1328 (ν^{s} —NO_2), 1424 (ν —N═N—). ^{1}H NMR (DMSO-d_6) δ_H ppm: 3.01 (d, 2H), 3.04 (d, 6H), 3.76 (s, 1H –OH), 6.78 (d 2H), 7.12 (d, 2H), 7.68 (d, 2H), 8.18 (d 1H), 8.40 (s 1H), 8.49 (s 1H), 8.80 (s, 1H), 9.66 (s, 1H —CH═N—). Elemental analysis calculated for $C_{22}H_{20}N_6O_5$: C, 58.92; H, 4.50; N, 18.74; O, 17.84, Found: C, 58.61; H, 4.96; N, 18.94; O, 17.21.

2.2.3. Preparation of 4-((1E)-(4-((4-(Dimethylamino)Benzylidene)Amino)-2-(Hydroxymethyl)Phenyl)Diazenyl)-3-Nitrobenzonitrile, ***AAM 3***

The AAM 3 was synthesized from 2 mmol (0.59 g) Azo-3 and 2.2 mmol (0.33 g) 4-(dimethylamino)benzaldehyde, yield 50%, m.p. 271–275 °C. ATR-FTIR cm^{-1}: 3457 and 3343 (ν –OH), 3217 (ν_{C-H} —CH═N—), 2232 (ν —C≡N), 1680 ($\nu_{C=N}$ —CH═N—), 1501 and 1335 (ν —NO_2), 1438 (ν —N—N—). ^{1}H NMR (DMSO-d_6), δ_H ppm: 2.99 (d, 2H), 3.04 (d, 6H), 4.43 (s, 1H —OH), 6.78 (d, 2H), 7.08 (d,

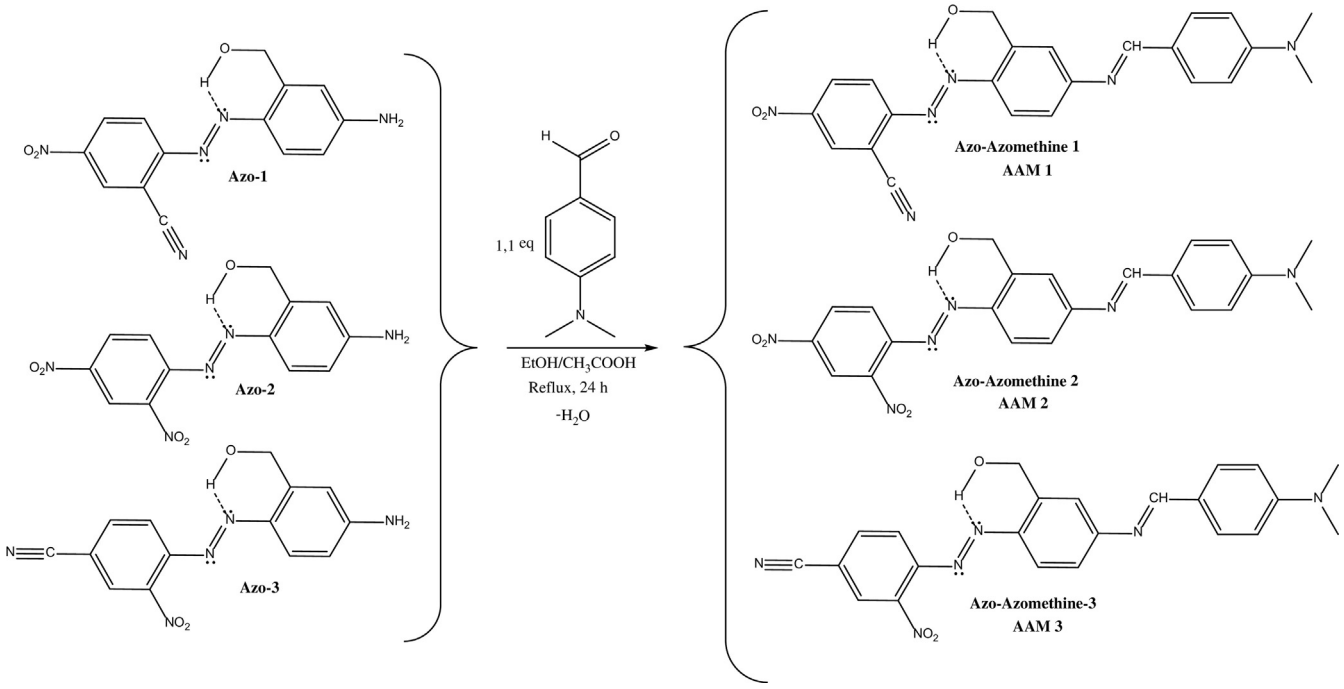

Scheme 1. Synthetic pathway for preparation of the azo-azomethine dyes (AAM 1, AAM 2 and AAM 3).

1H), 7.19 (d, 2H), 7.31 (s, 1H), 7.68 (d, 2H), 7.81 (s, 1H), 8.09 (s, 1H), 8.44 (d, 1H), 9.66 (s, 1H —CH═N—). Elemental analysis calculated for $C_{23}H_{20}N_6O_3$: C, 64.48; H, 4.71; N, 19.62; O, 11.20, Found: C, 64.34; H, 4.35; N, 19.36; O, 11.09

2.3. Quantum Chemical Calculations

The optimization of molecular geometry and electronic structure of studied molecules were performed by GAUSSIAN 09 W software package using density-functional theory DFT/B3LYP functional combined with the standard 6-311++G(d,p) basis set in vacuo [30]. The TD-DFT and Natural Bonding Orbital (NBO) were performed on optimized geometry of *trans (E)* and *cis (Z)* azo-azomethine dyes at the same basis set in vacuo. The frequency analysis was made at the same level of theory to characterize the stationary points on the potential surface and to obtain thermodynamic parameters such as absolute enthalpy (H) and Gibbs free energy (G) at 298 K. The precomputed vibrational scaling factor 0.967 was used according to the CCCBDB (Computational Chemistry Comparison and Benchmark Data Base) of National Institute of Standards and Technology, U.S. Department of Commerce [31].

2.4. Vapour Deposition of Nanosized Films

The thin films of AAM dyes were prepared by evaporation from Knudsen type vessels on quartz substrates with vacuum pressure 6×10^{-6} mbar. The temperature of evaporation was kept between 80 and 100 °C. Temperature of substrate was 11 °C, controlled by thermal regulator with Peltier element. The evaporation rate was 0.2–0.5 nm per *sec*. Sample thickness was 100 nm, as measured by Talystep profilometer with 10 nm accuracy.

2.5. Spectral Characterization

ATR-FTIR spectra of the compounds were recorded on a Bruker Tensor 27 FTIR spectrophotometer in the range 4400–600 cm^{-1} with resolution 2 cm^{-1} at room temperature. The external reflection diamond crystal has been used and the samples were scanned 128 times. The NMR spectra were collected on Bruker Avance II+ spectrometer with frequency 600 MHz in DMSO-d_6. The UV-VIS spectra have been measured on the Cary 5E-UV-VIS-NIR spectrophotometer. The calibration curves of the dyes were plotted by several points of absorption measurements in different concentrations and molar extinction coefficients (ε_{max}) in DMF were calculated.

2.6. Laser Induced Photoisomerization

The laser induced *trans-cis-trans* photoisomerization experiment was performed in DMF solution at room temperature on custom build optical setup equipped with high resolution spectrometer HR4000 (Ocean Optics) operating in the range 200–1100 nm. The light source is a halogen lamp (HL-2000). Its light is directed to the sample and then from the sample to the spectrometer by optical fibers. Special care is taken to eliminate all possible sources of stray light. The pump lasers at $\lambda = 355$ nm (output power 20 mW) and $\lambda = 491$ nm (output power 35 mW) were directed at small angle to the probe beam. After laser illumination the probes were relaxed 30 min in the dark. The spectra were collected at every 30 s during the entire experiment – illumination and dark relaxation. Before the experiments the solutions of the dyes were stored in the dark overnight.

3. Results and Discussion

3.1. Background of Interpretation of the Results

Three azo-azomethine (AAM) dyes were synthesized (see Scheme 1) containing donor and acceptor parts in order to investigate their photochromic and photodynamic behavior. The electron withdrawing (EW) and electron donating (ED) groups lead to unsymmetrical electron ("push-pull") distribution on the molecular backbone. The AAM-1 was synthesized by condensation reaction between 4-aminoazobenzene dye (Azo-1) with EW —C≡N at 2′-, —NO_2 at 4′-positions and 4-(dimetylamino)benzaldehyde. The AAM-2 was

designed with 4-aminoazobenzene dye (Azo-2) containing two EW -NO_2 groups at 2′- and 4′- positions via condensation reaction with 4-(dimetylamino)benzaldehyde. Finally, AAM-3 was synthesized with reversed positions of EW groups: 2′- NO_2 and 4′—C≡N. The optimized molecular geometry and thermodynamic parameters of the *trans (E)* and *cis (Z)* isomers were computed at DFT/B3LYP/6-311++G(d,p) level of theory in vacuo. The NBO (natural bond orbital) analysis was performed to evaluate the charge transfers (CT) and resonance energy on molecular backbone of *trans (E)* and *cis (Z)* of the dyes. The electron transitions spectra and excitation energies of *trans (E)* and *cis (Z)* isomers were calculated by TD-DFT in vacuo in order to understand the electron transitions and molecular contributions, which are referred to the experimental spectra of nanosized films of the dyes. The E_g (optical band gap energy) that defines the transition energy between frontier HOMO (highest occupied molecular orbital) and LUMO (lowest unoccupied molecular orbital) were computed and experimentally estimated by UV-VIS spectroscopy in nanosized films. The solvatochromic behavior was investigated in five different solvents with increasing polarity: 1,4-dioxane (non polar), THF (polar aprotic), n-BuOH (polar protic), acetone (polar aprotic) and DMF (polar aprotic) to estimate the influence of the polarity on electron transitions energy. The photoisomerization of the AAM chromophores was performed at room temperature with pump lasers at λ = 355 and 491 nm and in dark relaxation at equal concentrations and irradiation time.

3.2. Molecular Geometry, Quantum Mechanical TD-DFT Calculations and Solvatochromism

In order to find the structures with minimal energy E (RB3LYP), the different conformers of the AAM dyes were optimized as *trans (E)* and *cis (Z)* isomers. The optimized structures of the dyes are presented on Fig. 2. The synthesized dyes contain central phenyl rings, which is *para* substituted by —N═N— group with acceptor part and —CH═N— group with donor part. The hydroxymethylene (—CH_2OH) group in *ortho* place to the —N═N— group has a capacity to form an intramolecular six-membered ring hydrogen bonding with nonbonding electron pairs by the one of azo nitrogens. The molecular geometry of *trans (E)* isomers is linear non-planar, depending on the two chromophore groups. The —N═N— has near planar conformation with respect to the phenyl rings with dihedral angles N(10)═N(11)—C(12)—C(13) ~ 15–16° for AMM 1, ~30° for AAM 2 and AMM 3 due to the steric effect of *ortho* -NO_2 groups, while the —CH═N— has non-planar conformation with dihedral angle —C(4)—C(6)—N(25)═C(32) ~ 40° (Table 1). The geometry of *cis (Z)* isomers shows perpendicular orientation of —CH═N— and 4-(dimethylamino)phenyl rings to central phenyl rings with dihedral angles ~ 82–95°. The dihedral —N(10)═N(11)—C(12)—C(13)— angles for the three dyes are ~62–65°. However, the dihedrals —C(1)—N(10)═N(11)—C(12)— for AAM 2 and AAM 3 are ~17°, while for AAM 1 is ~10° due to the steric

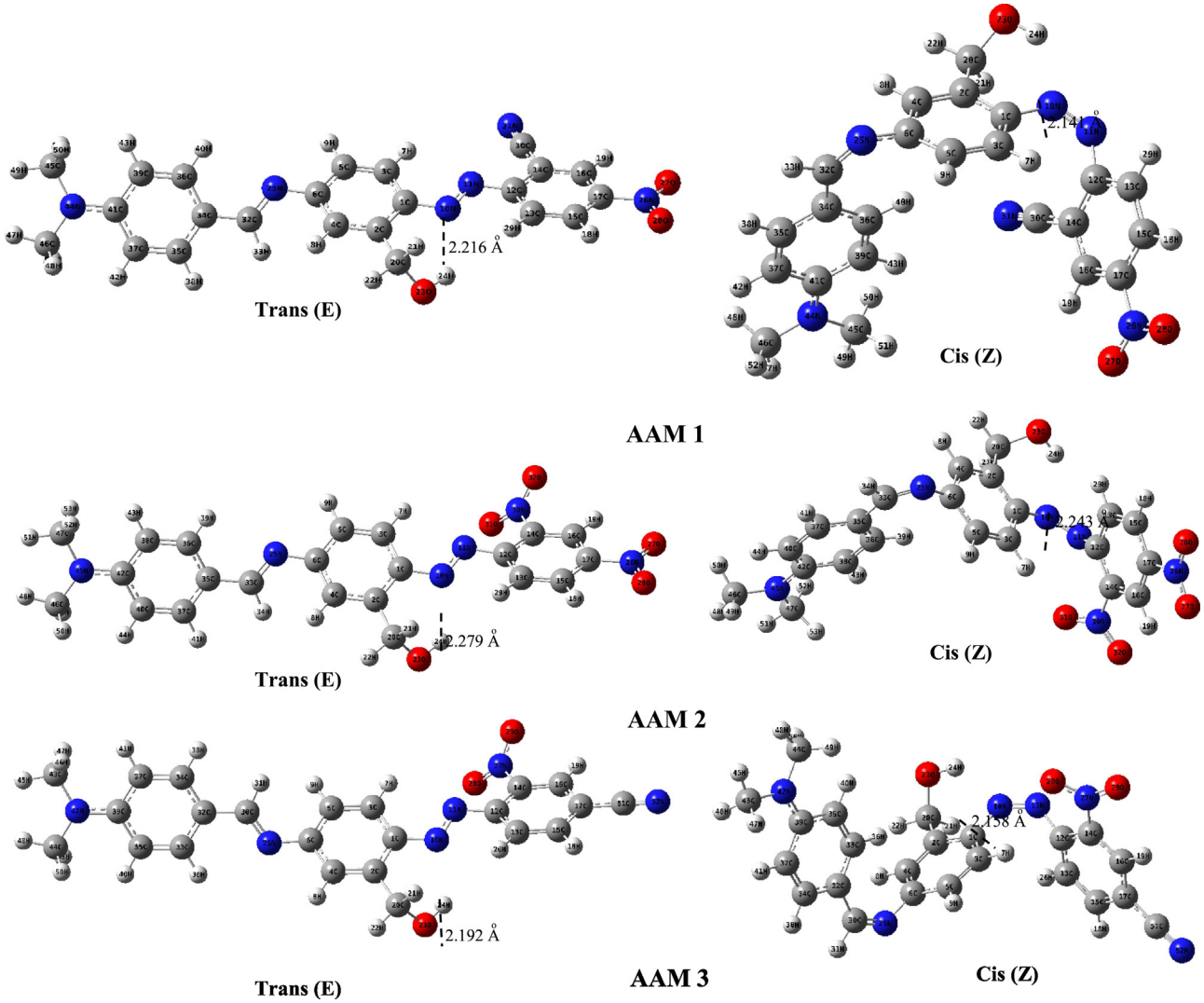

Fig. 2. Optimized molecular geometry of the AMM dyes as *trans (E)* and *cis (Z)* isomers by DFT/B3LYP/6-311++G(d,p) level of theory in vacuo.

Table 1
Theoretically calculated geometrical and bond parameters by DFT/B3LYP/6-311++G(d,p) level of theory in vacuo of the azo-azomethines.

Compounds	Dihedral angle via —N═N— bond [°]	Dihedral angle via —N═CH— bond [°]	Intramolecular H-bonding [Å]
trans (E) AAM 1	—C(1)—N(10)═N(11)—C(12)— 178.08 —N(10)═N(11)-C(12)-C(13)— −15.84	—C(6)—N(25)═C(32)-C(34)— 175.03 —C(4)—C(6)—N(25)═C(32)— −41.88	2.216
cis (Z) AAM 1	—C(1)—N(10)═N(11)—C(12)— 10.73 —N(10)═N(11)—C(12)—C(14)— 65.38	—C(6)—N(25)═C(32)—C(34)— 3.64 —C(4)—C(6)—N(25)═C(32)— 82.16	2.141
trans (E) AAM 2	—C(1)—N(10)═N(11)—C(12)— 176.33 —N(10)═N(11)—C(12)—C(13)— −30.46	—C(6)—N(25)═C(33)—C(35)— 174.27 —C(4)—C(6)—N(25)═C(33)— −41.91	2.279
cis (Z) AAM 2	—C(1)—N(10)═N(11)—C(12)— −17.52 —N(10)═N(11)—C(12)—C(13)— −62.23	—C(6)—N(25)═C(33)—C(35)— −0.44 —C(4)—C(6)—N(25)═C(33)— 95.23	2.243
trans (E) AAM 3	—C(1)—N(10)═N(11)—C(12)— 176.86 —N(10)═N(11)—C(12)—C(13)— −28.69	—C(6)—N(25)═C(30)—C(32)— 175.02 —C(5)—C(6)—N(25)═C(30)— −40.65	2.192
cis (Z) AAM 3	—C(1)—N(10)═N(11)—C(12)— 16.19 —N(10)═N(11)—C(12)—C(13)— 63.69	—C(6)—N(25)═C(30)—C(32)— 1.79 —C(5)—C(6)—N(25)═C(30)— 88.34	2.158

effect of *ortho* nitro groups of AAM 2 and AAM 3 (Table 1). The length of intramolecular hydrogen bonding is shorter in *cis (Z)* compared to the *trans (E)* isomers. In the *cis (Z)* isomers the n-π conjugation of non-bonding azo nitrogens electron pair with aromatic π-systems is decreased and it has great capacity to donate the electron density, as we will further discuss by NBO analysis.

Through DFT molecular geometry optimization and vibrational energy can be obtained important information to understand the photochromic and photodynamic behavior of the dyes. Table 2 presents the calculated total electronic energy *E (RB3LYP)* and dipole moment μ as well as thermodynamic parameters - absolute enthalpy H_{298} (sum of electronic and thermal enthalpies) and free Gibbs energy G_{298} (sum of electronic and thermal free Gibbs energies) of the AAM chromophores in *trans (E)* and *cis (Z)* isomers. The $\Delta E_{trans \rightarrow cis}$, $\Delta\mu_{trans \rightarrow cis}$, $\Delta H_{trans \rightarrow cis}$ and $\Delta G_{trans \rightarrow cis}$ were defined as difference between final state (f) *cis (Z)* isomers, which are products of the photochemical reaction and initial state (i) *trans (E) isomers,* which are reactants. The $\Delta H_{trans \rightarrow cis} > 0$ and $\Delta G_{trans \rightarrow cis} > 0$ show that $E \rightarrow Z$ isomerization is reversible photochemical reaction and does not occur spontaneously without UV irradiation to a less stable *cis (Z)* isomer. The $\Delta S_{trans \rightarrow cis}$ of AMM 1 and AMM 2 decreases, while for AAM 3 increases. The $\Delta S_{trans \rightarrow cis}$ is related to the order of the macroscopic system and probability of photoisomerization reactions to *cis (Z)* isomers. For AAM 3 the change of entropy has a positive value because of higher $\Delta H_{trans \rightarrow cis}$ compared to the $\Delta G_{trans \rightarrow cis}$. This indicates that AAM 3 is more stable in *trans (E)* isomers, while for AAM 1 and AMM 2 the photoisomerization to *cis (Z)* isomer is favored by the kinetic factor. These theoretical results have been confirmed later by experimental laser induced *trans-cis-trans* photoisomerization cycle. The molecular dipole moment is a vector sum of bond dipole moments and mainly depends on molecular geometry. Lower dipole moments in *cis (Z)* compared to *trans (E)* isomers means that the bonds polarity are decreased and the direction of vector dipoles of the bonds are opposite and canceled each other. The $\Delta\mu_{trans \rightarrow cis}$ values of AMM 1 and AAM 3 show significant decrease compared to the AAM 2 due to the polarization of the molecular backbone by the two EW $-NO_2$ groups. The computed and experimental values of vibrational bands of the chromophores are given in Supplementary Information Tables S.1, S.2 and S.3 and Figs. S.2, S.3 and S.4. The frequencies of the IR bands of ν —CH═N— for *cis (Z)* isomers are higher compared to the *trans (E)* isomers and synthesized dyes due to the decrease n-π and π-π conjugation with aromatic systems and increased force constant of the double bond.

Table 2
Theoretically calculated total electronic energy E (RB3LYP), dipole moment μ and thermodynamic parameters of *trans (E)* and *cis (Z)* isomers of the azo-azomethine dyes by DFT/B3LYP/6-311 + G(d,p) level of theory in vacuo.

Compounds	E (RB3LYP) [kcal mol^{-1}]	μ [D]	H_{298} [kcal mol^{-1}]	G_{298} [kcal mol^{-1}]	$\Delta E_{trans \rightarrow cis}$ [kcal mol^{-1}]	$\Delta\mu_{trans \rightarrow cis}$ [D]	$\Delta H_{trans \rightarrow cis}$ [kcal mol^{-1}]	$\Delta G_{trans \rightarrow cis}$ [kcal mol^{-1}]	[a]$\Delta S_{trans \rightarrow cis}$ [cal K^{-1} mol^{-1}]
trans(E) AAM 1	−905,426.6974	14.96	−905,158.0715	−905,217.9215	18.8455	−8.56	18.8309	19.1183	−0.9639
cis (Z) AAM 1	−905,407.8519	6.40	−905,139.2405	−905,198.8031					
trans(E) AAM 2	−975,888.9671	15.01	−975,617.5794	−975,679.4425	16.9591	−2.70	16.9509	17.1693	−0.7324
cis (Z) AAM 2	−975,872.008	12.31	−975,600.6285	−975,662.2731					
trans(E) AAM 3	−905,421.7562	13.91	−905,153.1148	−905,212.8474	16.5141	−4.01	16.5210	16.0680	1.5195
cis (Z) AAM 3	−905,405.242	9.90	−905,136.5937	−905,196.7794					

[a] $\Delta S = \frac{\Delta H - \Delta G}{T}$

The calculated bands of ν —N═N— for *trans (E)* isomers are in good agreement with the experimental spectra, whereas for the *cis (Z)* isomers are not or very weak registered due to the symmetric vibrations, where $(\frac{du}{dr})r_0 = 0$.

The natural charges of atoms in functional groups provide information about molecular polarizability, electronic structure and charge affects on dipole moment. The natural bond orbitals (NBO) analysis and second order Fock matrix are carried out by considering all possible interactions between (donor) Lewis NBOs and (acceptor) non Lewis NBOs. The intramolecular charge transfers (CT) or conjugations on molecular backbone are the main features of photochromic properties of the molecules. For each donor NBO (i) and acceptor NBO (j), the resonance stabilization energy associated with i → j delocalization can be evaluated as (Eq. 1),

$$E(2) = \Delta E_{ij} = q_i \frac{F(i,j)^2}{\varepsilon_j - \varepsilon_i} \quad (1)$$

where q_i is the donor orbital occupancy, ε_j and ε_i are diagonal elements and $F_{(i,j)}$ is the off diagonal NBO Fock matrix element [32,33]. The natural charges and NBOs analysis of azo-azomethine dyes are presented on Fig. 3 and Table 3.

The stabilization energy E(2) indicates the intensive interaction between electron donors and electron acceptors and increases with the extent of conjugation of the whole system in *trans (E)* isomers. The CT from π donor C32-C34 to π* acceptor N25-C30 and from π donor C1-

Table 3
Second order perturbation theory analysis of Fock matrix in NBO basis of azo-azomethine dyes calculated by DFT/B3LYP/6-311++G(d,p) level of theory in vacuo.

Compounds	Donor NBO (i)	Acceptor NBO (j)	E(2) [kcal mol^{-1}]	E(j)-E(i) [a.u]	F(i,j) [a.u]
trans (E) AAM 1	π C1-C2	π* N10-N11	26.76	0.24	0.068
	π N10-N11	π* C12-C14	10.23	0.34	0.059
	π N25-C30	π* C4-C6	11.35	0.381	0.032
	π C32-C34	π* N25-C30	23.14	0.21	0.067
cis (Z) AAM 1	π C1-C2	π* N10-N11	2.46	1.31	0.052
	π N10-N11	π* C12-C14	1.82	0.36	0.046
	π N25-C30	π* C4-C6	0.91	1.41	0.03
	π C32-C37	π* N25-C30	2.54	1.39	0.061
trans (E) AAM 2	π C1-C2	π* N10-N11	27.82	0.21	0.071
	π N10-N11	π* C12-C14	9.90	0.39	0.023
	π N25-C33	π* C5-C6	11.65	0.35	0.062
	π C35-C37	π* N25-C33	23.17	0.027	0.075
cis (Z) AAM 2	π C1-C2	π* N10-N11	2.41	1.35	0.051
	π N10-N11	π* C12-C14	0.76	0.21	0.012
	π N25-C33	π* C5-C6	0.51	0.89	0.056
	π C35-C37	π* N25-C33	0.76	1.35	0.029
trans (E) AAM 3	π C1-C2	π* N10-N11	27.22	0.21	0.071
	π N10-N11	π* C12-C14	11.06	0.38	0.063
	π N25-C30	π* C4-C6	11.52	0.36	0.04
	π C32-C34	π* N25-C30	23.11	0.27	0.74
cis (Z) AAM 3	π C1-C2	π* N10-N11	2.75	1.27	0.053
	π N10-N11	π* C12-C14	2.73	0.38	0.032
	π N25-C30	π* C4-C6	0.94	1.44	0.033
	π C32-C37	π* N25-C30	2.76	1.32	0.054

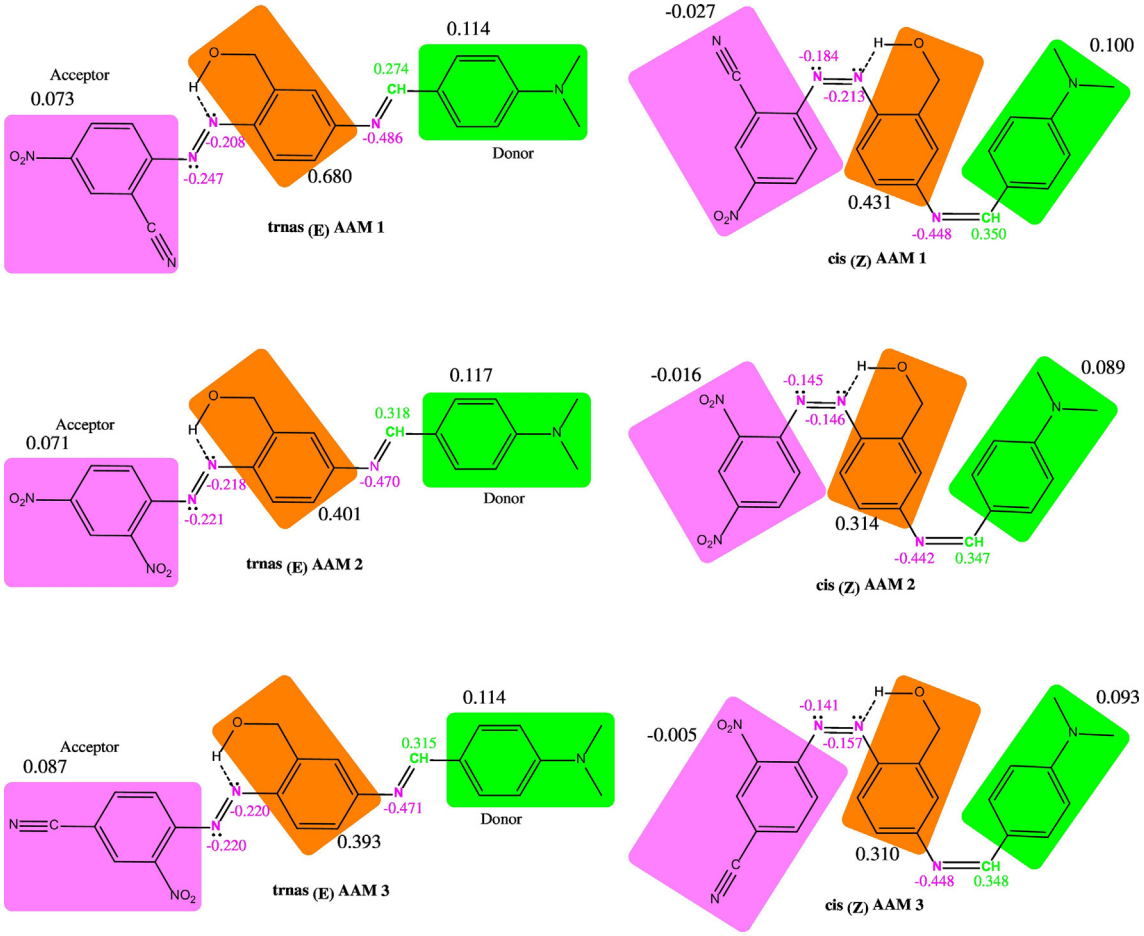

Fig. 3. NBO charges of *trans (E)* and *cis (Z)* isomers of the AAM dyes calculated at DFT/B3LYP/6-311++G(d,p) level of theory in vacuo. Charge transfer on molecular backbones is presented by summing the atoms charges in different colored part in molecules. The charges distribution are marked as donor and acceptor parts of the dyes connected via azo and azomethine bridges with central phenyl ring.

C2 to π* acceptor N10-N11 is characterized by high resonance energy, which shows effective π-π conjugation of —CH═N— and —N═N— groups in *trans (E)* isomers of the dyes. In the *cis (Z)* isomers the resonance energy significantly decreases, because of changes of the geometry (two phenyl rings are twisted in respect to the C—N═N—C and near perpendicular orientation of —CH═N— and 4-(dimethylamino)phenyl rings to the central phenyl ring) and orbital symmetry of the molecule, which indicate strong decrease of π-π conjugation. This shows that the AAM dyes are more stable in *trans (E)* isomers, because of higher energy of resonance stabilization and effective π-π conjugation (Table 3). The summing of the atoms charges on acceptor, donor and central phenyl rings indicated great donor-acceptor electron transfer of the *trans (E)* isomers (Fig. 3). The AAM 1 and AAM 2 with *para* substituted $-NO_2$ groups have stronger accepting properties compared to the AAM 3 with *para* –CN group. Due to the increasing electron flow from donor to acceptor the dipole moment (μ) is higher one (Table 3). The *cis (Z)* isomers are characterized by significant decrease of electron density on acceptor parts. The non-effective conjugation is also confirmed by decrease of atomic charges of chromophore groups.

The investigation of the electronic spectral features of the AMM dyes is important in order to estimate the electron transitions energy, optical band gap and HOMO-LUMO energy levels of frontier orbitals. Quantum mechanics determines the properties of nanomaterials with one dimension in the range 1 to 100 nm, and calculation methods to deal with nanomaterials are being developed. When one or more dimensions of a material are below 100 nm, especially below 20 nm, dramatic changes can occur in the optical, electronic, chemical, and other properties compared with those of the bulk material [34]. The reason is behavior of the materials close to the properties of single molecule in vacuo. The electronic spectra (vertical transition and excitation energy) of *trans (E)* and *cis (Z)* AAM dyes calculated by TD-DFT after geometry optimization by B3LYP/6-311++G(d,p) level of theory in vacuo and experimental spectra of the vapour deposited nanosized films with 100 nm thicknesses are presented on Fig. 4. The electron transitions energy and

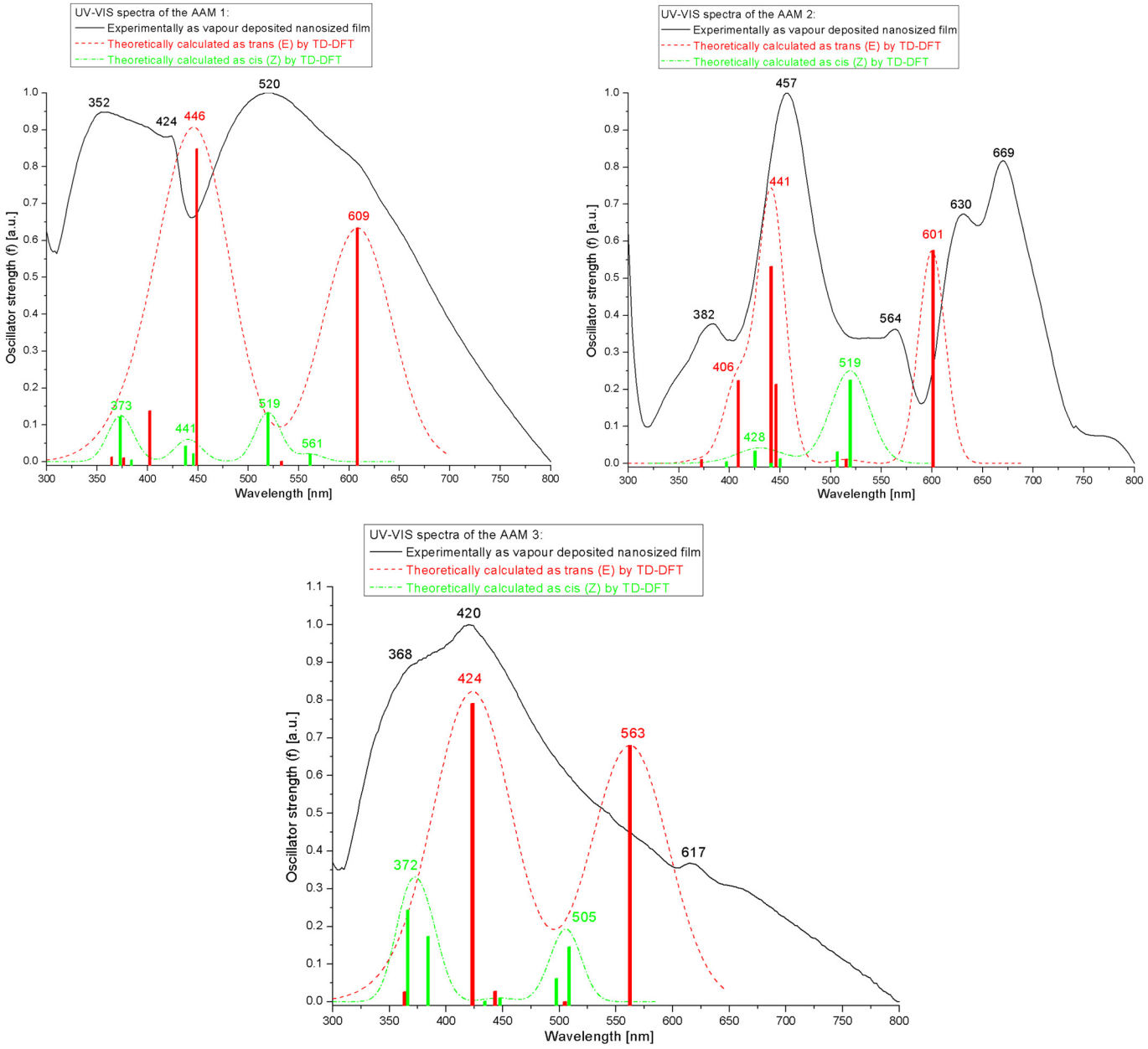

Fig. 4. TD-DFT calculated UV-VIS spectra of the *trans (E)* and *cis (Z)* azo-azomethine dyes by B3LYP/6-311++G(d,p) level of theory in vacuo. The theoretical spectra were correlated with the spectra of the vapour deposited nanosized films with 100 nm thickness of the synthesized AAM 1, AAM 2 and AAM 3.

molecular contributions are given in Supplementary Information Tables S.4, S.5, S.6, S.7, S.8, S.9.

The TD-DFT spectrum of AAM 1 as *trans (E)* isomer shows strong electron transitions, which refers to the λ_{max} = 609 nm HOMO → LUMO (n → π*) and λ_{max} = 446 nm HOMO-1 → LUMO (π → π*). The spectrum of the nanosized vapour deposited film is characterized by two absorption maxima in the UV range at λ_{max} = 352 and 424 nm. It can be assumed that λ_{max} = 352 nm refers to the HOMO → LUMO + 1, where in the theoretical spectrum this transition appears at λ_{max} = 405 nm with small *f* (oscillator strength) compared to the HOMO → LUMO and HOMO-1 → LUMO transitions (Table S.4.). In the VIS range of the experimental spectrum broad absorbance band is observed with λ_{max} = 520 nm. The hypsochromic (blue shift) and hypochromic effects are observed in the computed electronic spectrum as *cis (Z)* isomer (λ_{max} = 561 nm HOMO → LUMO for —N═N— n → π*, λ_{max} = 519 nm HOMO-1 → LUMO for —CH═N— n → π* and λ_{max} = 441 nm HOMO-2 → LUMO, π → π*). These indicate the forbidden symmetry of the frontier molecular orbitals and the other indirect transition are allowed HOMO-2 → LUMO, HOMO-1 → LUMO + 1 (Table S.5). The AAM 2 as *trans (E)* isomer of calculated UV-VIS spectrum has absorption maximum with strong *f* in the VIS range λ_{max} = 601 nm HOMO → LUMO (n → π*). The UV range is characterized by absorption maximum at λ_{max} = 441 nm HOMO → LUMO + 1 and HOMO-1 → LUMO for π → π* with shoulder at λ_{max} = 406 nm HOMO → LUMO + 1 and HOMO-3 → LUMO for π → π* of *ortho* NO_2 group (Table S.6). The experimental spectra of nanosized film of AAM 2 has splitting band in VIS range at λ_{max} = 630 and 669 nm probably due to π-π stacking. The λ_{max} in UV range 457 and 382 nm have a good fit with calculated spectrum of the *trans (E)* isomer. The *cis (Z)* TD-DFT spectrum is also characterized with blue shift and hypochromic effect compared to the *trans (E)* spectrum (Table S.7). The theoretical spectrum of the *trans (E)* AAM 3 mainly is characterized by two vertical electron transitions HOMO → LUMO, n → π (λ_{max} = 563 nm) and HOMO → LUMO + 1, π → π (λ_{max} = 424 nm). The other transitions have insignificant contribution on the absorption spectrum (Table S.8). The experimental spectrum has long absorption tail in the VIS range with λ_{max} = 617 nm. The UV range has one broad band at λ_{max} = 420 nm with shoulder at λ_{max} = 368 nm. The correlation between TD-DFT calculated and experimental spectra of nanosized films of the AAM dyes is useful to understand the energy of electron transitions of the frontier orbitals. From practical point of view this can be applied for development of light driven optical switches, reversible optical storage, solar cell materials and others photonics applications.

In organic molecules, the energy levels of the electronic states correspond to the energy carried by UV or VIS radiation. At resonance, the molecules can absorb quantified energy transported by the electromagnetic radiation, and promote an electron from the low energy molecular orbital to the higher one [35]. These transitions can be measured using a UV-VIS spectrophotometer, where E_g corresponds to the energy of the long wavelength edge of the excitation absorption band [36,37]. The longest absorption wavelength λ_{onset} is used to calculate the optical gap energy, E_g, according to the eq. 2 [35]:

$$E_g = h.\nu = \frac{h.c}{\lambda} = \frac{1242}{\lambda} \quad (2)$$

Table 4
Theoretically calculated HOMO and LUMO energy levels of frontier orbitals and experimentally determined E_g as nanosized films of the *trans (E)* AAM compounds.

Compounds	Theoretically calculated [eV]			Absorption edge [nm]	Experimentally determined E_g [eV]
	HOMO	LUMO	E_g		
AMM 1	−5.91	−3.67	2.24	796	1.56
AAM 2	−5.91	−3.61	2.27	798	1.55
AAM 3	−5.87	−3.43	2.43	794	1.56

Table 5
Experimentally calculated solvatochromic shifts (Δλ), molar extinctions in DMF (ε_{max}) of the AAM chromophores in different polar solvents.

Compounds	λ_{max} [nm]					Δλ [nm]	ε_{max} [L mol^{-1} cm^{-1}] in DMF
	1,4-Dioxane	THF	n-BuOH	Acetone	DMF		
AAM 1	334	340	339	337	361	27	205,551.94
	431	421	501	495	504	73	(λ_{max} 361 nm)
AAM 2	332	334	336	335	342	10	43,027.64
	384	392	390	389	394	10	(λ_{max} 342
	468	485	556	483	502	34	nm)
AAM 3	330	332	341	335	338	8	28,246.87
	372	379	387	386	382	10	(λ_{max} 338
	480	490	531	513	529	49	nm)

The theoretically calculated HOMO and LUMO energy levels and E_g of the dyes are close, which determines the absorption maxima in VIS range. The experimentally determined E_g of nanosized films are also similar, but approximately 0.7 eV lower in energy compared to the theoretical (Table 4).

Solvatochromism was also assessed by UV-VIS absorption spectra in five different solvents (1,4-dioxane, THF, n-BuOH, acetone and DMF) with increasing polarity (Table 5 and Fig. 5). The AAM 1 and AAM 2 dyes exhibit a red (bathochromic) shift, which shows a decrease of electron transition energy as solvent polarity increases. The AAM 3 has highest shifting in n-BuOH (polar protic) due to the intermolecular H-bonding between solvent and dye (λ_{max} = 341, 387 and 531 nm). The extinction coefficient ε_{max} were determined in DMF, which decrease in order AAM 1 > AAM 2 > AAM 3. The AAM 1 has biggest solvatochromic shift, while the AAM 3 smallest (Table 5). The AAM 2 and AMM 3 show significant absorption (hyperchromic effect) in acetone in the VIS range, where the n → π* transitions appear (AAM 2 λ_{max3} = 483 nm, AAM 3 λ_{max3} = 513 nm). The shoulder at λ_{max2} = 384 nm (in 1,4-dioxane for AAM 2) and λ_{max2} = 372 nm (in 1,4-dioxane for AAM 3) is due to the competitive electron resonance distributions between azo π system and *ortho* nitro groups related to the indirect electron transitions (Table S.6 and S.8). The electron transitions π → π* and n → π* bands of all dyes are well separated due to the unsymmetrical electron distributions ("push-pull") of ED and EW groups (Fig. 5).

3.3. A Laser Induced Trans-Cis-Trans Photoisomerization.

In order to observe the photodynamic properties of the dyes, a laser-induced *trans-cis-trans* photoisomerization experiment was performed in DMF solution, in which the dyes exhibit strong solvatochromism, respectively low optical band gap (direct HOMO-LUMO transition energy). The photoisomerization is an important characteristic of azo-azomethines and the energy of this conversion depends on the previously discussed parameters - solvatochromism, E_g, and by energy and intensity of the UV light and time of irradiation. The experiments were conducted at identical concentrations and time of illumination in DMF. The aim was to evaluate the photodynamic properties of the chromophores in relation to the energy of the electron transitions. The degree of photoisomerization at the photostationary state, *R*, was evaluated according to the equation (Eq. 3) [38]:

$$R = \frac{(A_0 - A_\infty)}{A_0} \times 100 \quad (3)$$

where A_0 is the initial absorbance and A_∞ is the absorbance at the photostationary state.

The degree of E → Z photoisomerization was measured by real time UV-VIS absorption during illumination with laser pump at 355 nm for 30 min, while for the reversible Z → E relaxation with laser pump at 491 nm for 30 min. Finally, the spectra in dark relaxation for 30 min

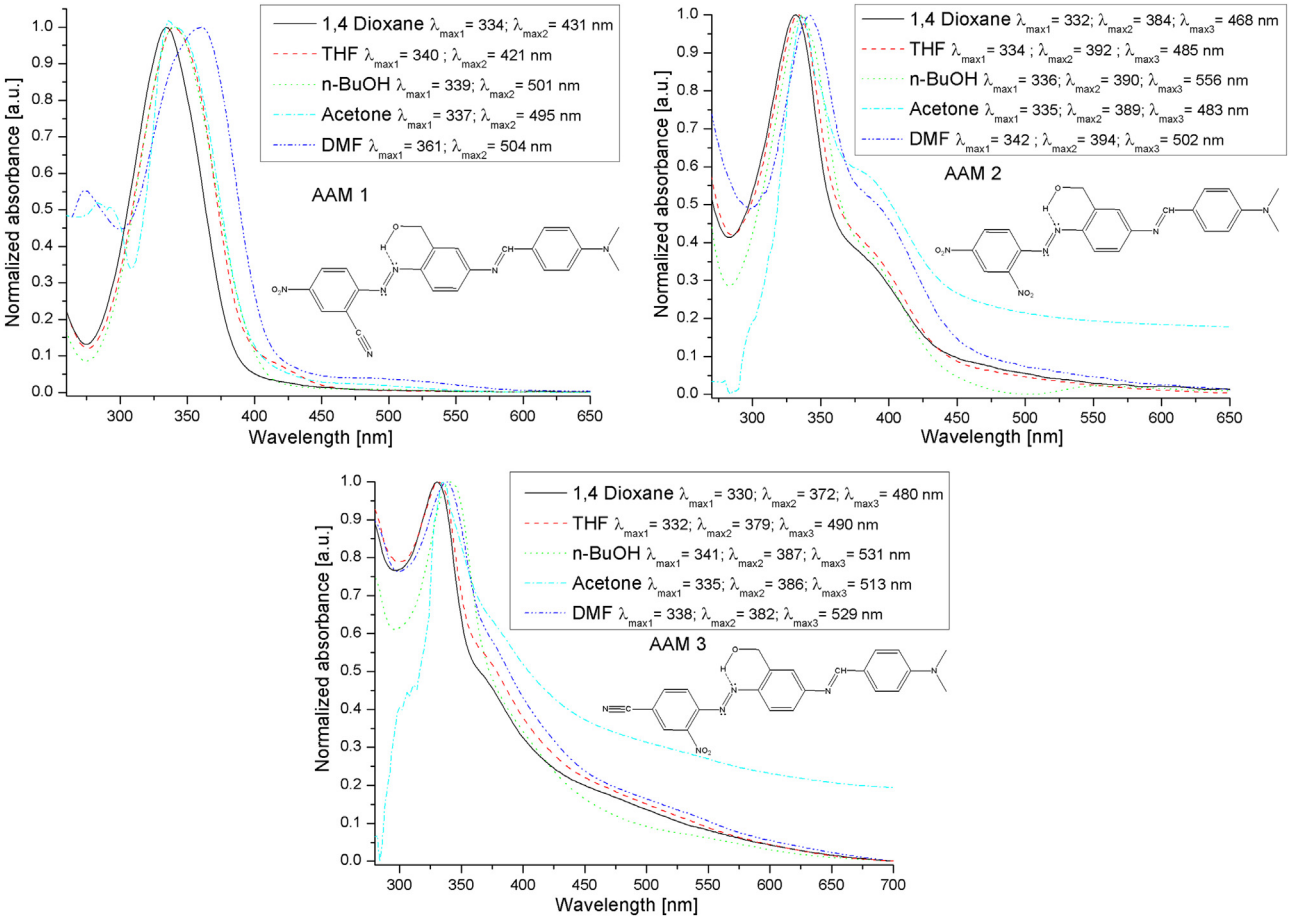

Fig. 5. Normalized UV-VIS spectra of the azo-azomethine dyes in 1,4-dioxane, THF, n-BuOH, acetone and DMF solutions.

have been measured. The representation of photoisomerization is given on Fig. 6 as function of the time and wavelength in the VIS range, where the changes are related to the direct HOMO-LUMO electron transitions ($n \rightarrow \pi^*$) of the dyes.

During the initial exposure at 355 nm fast E → Z conversion is registered for 600 s of the AAM 1. The photostationary states of conversion of the AAM 2 was achieved for 2000 s illumination, while for AAM 3 was 2150 s. Due to the photostationary equilibrium and thermodynamically more stable *trans (E)* isomers, a complete *cis (Z)* conversion cannot be achieved, although AAM 2 attained a degree of photoisomerization as high as 70%. The degree of E → Z photoisomerization of the AAM 1 and AAM 3 is 22 and 30%. The reversible Z → E relaxation at 491 nm exposure was achieved after 1500 s for AAM 1 and 300 s for AAM 3. The complete Z → E conversion of the $n \rightarrow \pi^*$ transitions of the AMM 1 ($\lambda_{max} = 504$ nm) and AAM 3 ($\lambda_{max} = 529$ nm) was achieved in the dark. The results also show that on 491 nm laser illumination and in the dark, the Z → E relaxation of the AAM 2 occurred at a significantly slower rate than in the other dyes, therefore it was possible to retain its predominant *cis (Z)* isomer for an extended period of time. The absorption of the $n \rightarrow \pi^*$ transitions in the VIS range in polar DMF solvent increases during conversion from *trans (E)* to *cis (Z)* isomer by pump laser at 355 nm for AAM 1 and AAM 3. For AAM 2 this change is insignificant, because of small change of dipole moment and large polarization effect of the two $-NO_2$ groups. The reversible Z → E reaction by exposure at 491 nm and in the dark shows the decrease of absorption (AAM 1 and AAM 3) due to the symmetry-forbidden transition and six-membered intramolecular hydrogen bonding [39]. The results are in good agreement with theoretical calculated thermodynamically parameters, where the $\Delta S_{trans \rightarrow cis}$ of AMM 1 and AMM 2 has negative values, while for AAM 3 is positive. This indicates that AAM 3 is more stable in *trans (E)* isomer, while for AAM 1 and AMM 2 the photoisomerization to *cis (Z)* isomer is favored by the kinetic factor. The kinetic of *trans-cis-trans* photoisomerization cycle describes the photochromic and photodynamic properties of the dyes. As a result, azo and azomethine containing dyes have become an object of research interest and have been incorporated in various applications. The fast Z → E conversion can be applied as nanoscale molecular switches, while the slower rate of conversion can be used as optical data storage and dynamic holography.

4. Conclusions

Three azo-azomethine dyes (AAM 1, AAM 2 and AAM 3) containing donor and acceptor parts with existing intramolecular hydrogen bond between the $-CH_2OH$ and —N═N— groups have been synthesized. The optimized molecular geometry of *trans (E)* and *cis (Z)* isomers was computed at DFT/B3LYP/6-311++G(d,p) level of theory in vacuo. In the *trans (E)* isomers, —N═N— has near planar conformation with respect to the phenyl rings, while the —CH═N— has non-planar conformation. The perpendicular orientation of —CH═N— and 4-(dimethylamino)phenyl rings to the central phenyl rings of *cis (Z)* isomers has been found with minimal energy. The NBO analysis has shown that the charge transfer from π donor to π* acceptor is characterized by high resonance energy, which indicates effective π-π conjugation of —CH═N— and —N═N— groups in *trans (E)* isomers of the dyes. In the *cis (Z)* isomers the resonance energy significantly decrease, because of changes of the geometry and orbital symmetry of the molecule, which indicate strong decrease of π-π conjugation.

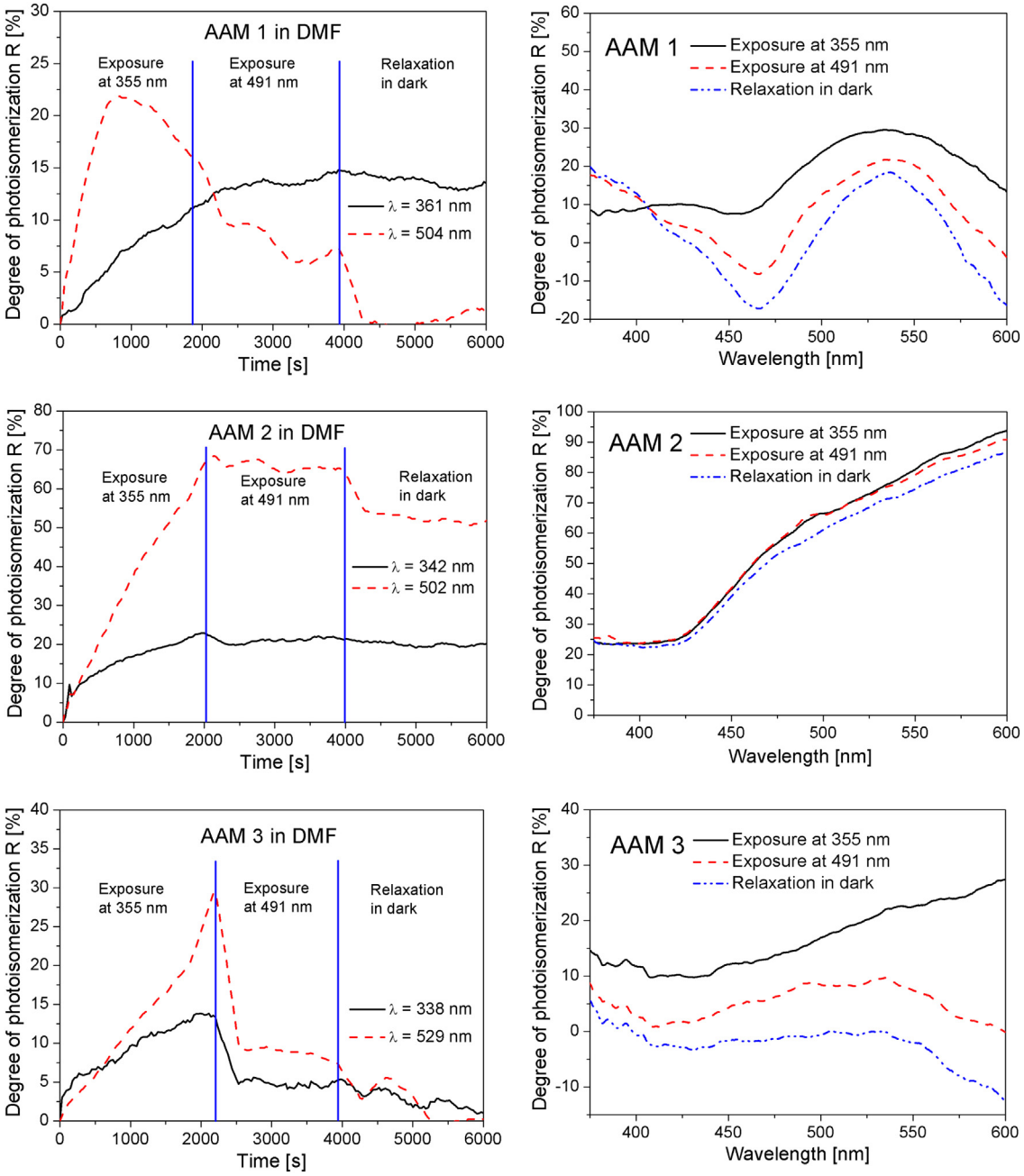

Fig. 6. Photoinduced *trans-cis-trans* photoisomerization cycle by pump lasers at λ = 355 (E → Z), 491 nm (Z → E) and relaxation in dark. The degree of photoisomerization was presented as function of the time of illumination and wavelength.

The TD-DFT calculated electronic spectra and energy of electron transitions of the frontier orbitals were correlated with the experimental UV-VIS spectra of the vapour deposited nanosized films. The experimental spectra are in good agreement with theoretically calculated *trans (E)* isomers. Solvatochromic behavior was investigated by UV-VIS absorption spectra in five different solvents (1,4-dioxane, THF, n-BuOH, acetone and DMF) with increasing polarity. The AAM 1 and AAM 2 dyes exhibit a red (bathochromic) shift, which shows a decrease of electron transition energy as solvent polarity increases. The AAM 3 has highest shifting in n-BuOH (polar protic) due to the intermolecular H-bonding between solvent and dye.

The calculated thermodynamic parameters $\Delta E_{trans \rightarrow cis}$, $\Delta\mu_{trans \rightarrow cis}$, $\Delta H_{trans \rightarrow cis}$, $\Delta G_{trans \rightarrow cis}$ and $\Delta S_{trans \rightarrow cis}$ have shown that $E \rightarrow Z$ isomerisation is reversible photochemical reaction and does not occur spontaneously without UV irradiation to a less stable *cis (Z)* isomer. The $\Delta S_{trans \rightarrow cis}$ of AMM 1 and AMM 2 decreases, while for AAM 3 increases. Through laser induced *trans-cis-trans* photoisomerization cycle the photochromic and photodynamic properties of the dyes have been describes. The degree of E → Z photoisomerization by laser pump at 355 nm is highest for AAM 2 (70%), while for AAM 1 and AAM 3 is 22 and 30%. The reversible Z → E relaxation at 491 nm exposure was achieved after 1500 s for AAM 1 and 300 s for AAM 3. The results was also shown that in 491 nm laser illumination and in the dark, the Z → E relaxation of AAM 2 occurs at a significantly slower rate than the other dyes, therefore it was able to retain its predominant *cis (Z)* isomer for an extended period of time. The results are in good agreement with theoretically calculated thermodynamic parameters, where the $\Delta S_{trans \rightarrow cis}$ of AMM 1 and AMM 2 has negative values, while for AAM

3 is positive. This indicates that AAM 3 is more stable in *trans (E)* isomers, while for AAM 1 and AMM 2 the photoisomerization to *cis (Z)* isomer and reversible reaction is favored by the kinetic factor.

Conflict of Interest

The authors declared that the article content has no conflicts of interest.

Acknowledgments

This work was financial supported by the Bulgarian National Scientific Fund project ДН 08/10 of the Ministry of Education and Science, Bulgaria and UCTM contract 11734. The authors gratefully acknowledge the Centre of Mathematical Modeling and Numerical Simulation at University of Chemical Technology and Metallurgy and MADARA cluster for computational time.

Appendix A. Supplementary data

Supplementary data to this article can be found online at https://doi.org/10.1016/j.saa.2017.11.016.

References

[1] Paulo J. Coelhoa, M. Cidália, R. Castrob, M. Manuela M. Raposob, Reversible trans–cis photoisomerization of new pyrrolidene heterocyclic imines, J. Photochem. Photobiol. A Chem. 259 (2013) 59–65, https://doi.org/10.1016/j.jphotochem.2013.03.004.
[2] Paulo J. Coelho, Céu M. Sousa, M. Cidália, R. Castro, A. Maurício, C. Fonseca, M. Manuela, M. Raposo, Fast thermal cis–trans isomerization of heterocyclic azo dyes in PMMA polymers, Opt. Mater. 35 (2013) 1167–1172, https://doi.org/10.1016/j.optmat.2013.01.007.
[3] Leif R. Knöpke, Anke Spannenberg, Angelika Brückner, Ursula Bentrup, The influence of substituent effects on spectroscopic properties examined on benzylidene aniline-type imines, Spectrochim. Acta A Mol. Biomol. Spectrosc. 95 (2012) 18–24, https://doi.org/10.1016/j.saa.2012.04.047.
[4] Liyan Zhao, Qiufei Hou, Dan Sui, Yue Wang, Shimei Jiang, Multistate/multifunctional switches based on photochromic Schiff base, Spectrochim. Acta A Mol. Biomol. Spectrosc. 67 (2007) 1120–1125, https://doi.org/10.1016/j.saa.2006.09.033.
[5] Haluk Dinc, Sinem Yavuza, Özgül Haklı, Ceylan Zafer, Cihan Özsoy, I•nci Durucasu, Sıddık I•cli, Optical and photovoltaic properties of salicylaldimine-based azo ligands, J. Photochem. Photobiol. A Chem. 210 (2010) 8–16, https://doi.org/10.1016/j.jphotochem.2009.12.012.
[6] Hamid Khanmohammadi, Khatereh Rezaeian, Thermally stable water insoluble azo-azomethine dyes: synthesis, characterization and solvatochromic properties, Spectrochim. Acta A Mol. Biomol. Spectrosc. 97 (2012) 652–658 10.1016/j.saa.2012.07.013.
[7] Hamid Khanmohammadi, Malihe Erfantalab, New 1,2,4-triazole-based azo-azomethine dyes. Part I: synthesis, characterization and spectroscopic studies, Spectrochim. Acta A Mol. Biomol. Spectrosc. 86 (2012) 39–43, https://doi.org/10.1016/j.saa.2011.09.053.
[8] Hamid Khanmohammadi, Malihe Erfantalab, Atena Bayat, Ali Babaei, Masoud Sohrabi, New 1,2,4-triazole-based azo–azomethine dyes. Part II: synthesis, characterization, electrochemical properties and computational studies, Spectrochim. Acta A Mol. Biomol. Spectrosc. 97 (2012) 876–884, https://doi.org/10.1016/j.saa.2012.07.041.
[9] Qinghua Wang, Lizhen Cai, Fei Gao, Qiurong Zhou, Fengping Zhan, Qingxiang Wang, Photochromism of Schiff base compounds derived from N,N'-bis(2-aminophenyl)isophthalamide: structure and photosensitivity, J. Mol. Struct. 977 (2010) 274–278, https://doi.org/10.1016/j.molstruc.2010.06.008.
[10] Malihe Erfantalab, Hamid Khanmohammadi, New 1,2,4-triazole-based azo–azomethine dye. Part III: synthesis, characterization, thermal property, spectrophotometric and computational studies, Spectrochim. Acta A Mol. Biomol. Spectrosc. 125 (2014) 345–352, https://doi.org/10.1016/j.saa.2014.01.113.
[11] Esin Ispir, The synthesis, characterization, electrochemical character, catalytic and antimicrobial activity of novel, azo-containing Schiff bases and their metal complexes, Dyes Pigments 82 (2009) 13–19, https://doi.org/10.1016/j.dyepig.2008.09.019.
[12] Hamid Khanmohammadi, Maryam Darvishpour, New azo ligands containing azomethine groups in the pyridazine-based chain: synthesis and characterization, Dyes Pigments 81 (2009) 167–173, https://doi.org/10.1016/j.dyepig.2008.07.019.
[13] Tao Tao, Feng Xu, Xiao-Chun Chen, Qian-Qian Liu, Wei Huang, Xiao-Zeng You, Comparisons between azo dyes and Schiff bases having the same benzothiazole/phenol skeleton: syntheses, crystal structures and spectroscopic properties, Dyes Pigments 92 (2012) 916–922, https://doi.org/10.1016/j.dyepig.2011.09.008.
[14] Iran Sheikhshoaie, Walter M.F. Fabian, Quantum chemical study on the electronic structure and second-order nonlinear optical properties of salen-type Schiff bases, Dyes Pigments 70 (2006) 91–98, https://doi.org/10.1016/j.dyepig.2005.04.011.
[15] Ying Qian, Gang Wang, Guomin Xiao, Baoping Lin, Yiping Cui, The first-order molecular hyperpolarizability and thermal stability of charge-transfer azo diol and azo aldimine, Dyes Pigments 75 (2007) 460–465, https://doi.org/10.1016/j.dyepig.2006.06.029.
[16] H.M. Dhammika Bandara, Shawn C. Burdette, Photoisomerization in different classes of azobenzene, Chem. Soc. Rev. 41 (2012) 1809–1825, https://doi.org/10.1039/C1CS15179G.
[17] Kevin G. Yager, Christopher J. Barrett, in: Yue Zhao, Tomiki Ikeda (Eds.), Azobenzene Polymers for Photonic Applications, Book chapter in Smart Light-Responsive Materials, John Wiley & Sons, Inc. 2009, pp. 1–27 (ISBN: 978-0-470-17578-1).
[18] Ying Luo, Manuel Utecht, Jadranka Dokic, Sergey Korchak, Hans-Martin Vieth, Rainer Haag, Peter Saalfrank, Cis–trans isomerisation of substituted aromatic imines: a comparative experimental and theoretical study, ChemPhysChem 12 (2011) 2311–2321, https://doi.org/10.1002/cphc.201100179.
[19] H.L. Saadon, Basil Ali, Adil A. Al-Fregi, Nonlinear optical properties of new organotellurium compounds containing azomethine and azo groups under CW laser illumination, Opt. Laser Technol. 58 (2014) 33–38, https://doi.org/10.1016/j.optlastec.2013.10.032.
[20] Alexander V. Gaenko, Ajitha Devarajan, Laura Gagliardi, Roland Lindh, Giorgio Orlandi, Ab initio DFT study of Z–E isomerization pathways of N–benzylideneaniline, Theor. Chem. Accounts 118 (2007) 271–279, https://doi.org/10.1007/s00214-007-0319-1.
[21] Jayaraman Jayabharathi, Venugopal Thanikachalam, Marimuthu Venkatesh Perumal, Natesan Srinivasan, A physiochemical study of azo dyes: DFT based ESIPT process, Spectrochim. Acta A Mol. Biomol. Spectrosc. 83 (2011) 200–206, https://doi.org/10.1016/j.saa.2011.08.017.
[22] M.R. Lutfor, G. Hegde, S. Kumar, C. Tschierske, V.G. Chigrinov, Synthesis and characterization of bent-shaped azobenzene monomers: guest–host effects in liquid crystals with azo dyes for optical image storage devices, Opt. Mater. 32 (2009) 176–183, https://doi.org/10.1016/j.optmat.2009.07.006.
[23] Sevgi Eskikanbur, Koray Sayin, Muhammet Kose, Huseyin Zengin, Vickie McKee, Mukerrem Kurtoglu, Synthesis of two new azo-azomethines; spectral characterization, crystal structures, computational and fluorescence studies, J. Mol. Struct. 1094 (2015) 183–194, https://doi.org/10.1016/j.molstruc.2015.03.043.
[24] Hamid Khanmohammadi, Khatereh Rezaeian, Mostafa M. Amini, Seik Weng Ng, Azo-azomethine dyes with N, O, S donor set of atoms and their Ni(II) complexes: Synthesis, characterization and spectral properties, Dyes Pigments 98 (2013) 557–564, https://doi.org/10.1016/j.dyepig.2013.03.023.
[25] Mario Amati, Carlo Bonini, Maurizio D'Auria, Maria Funicello, Francesco Lelj, Rocco Racioppi, Synthesis of heteroaryl imines: theoretical and experimental approach to the determination of the configuration of C═N double bond, J. Organomet. Chem. 71 (2006) 7165–7179, https://doi.org/10.1021/jo0605501.
[26] H. Shokry, Molecular dynamics simulation and quantum chemical calculations for the adsorption of some Azo-azomethine derivatives on mild steel, J. Mol. Struct. 1060 (2014) 80–87, https://doi.org/10.1016/j.molstruc.2013.12.030.
[27] Lukasz Hamryszak, Henryk Janeczek, Ewa Schab-Balcerzak, New thermotropic symmetrical and unsymmetrical azomethine with azobenzene unit and fluorinated alkyl chain: synthesis and characterization, J. Mol. Liq. 165 (2012) 12–20, https://doi.org/10.1016/j.molliq.2011.10.001.
[28] Chinnaiyan Selvarasu, Palaninathan Kannan, Effect of azo and ester linkages on rod shaped Schiff base liquid crystals and their photophysical investigations, J. Mol. Struct. 1125 (2016) 234–240, https://doi.org/10.1016/j.molstruc.2016.06.081.
[29] Anton Georgiev, Emil Bubev, Deyan Dimov, Denitsa Yancheva, Ivaylo Zhivkov, Jozef Krajčovič, Martin Vala, Martin Weiter, Maria Machkova, Synthesis, structure, spectral properties and DFT quantum chemical calculations of 4-aminoazobenzene dyes. Effect of intramolecular hydrogen bonding on photoisomerization, Spectrochim. Acta A Mol. Biomol. Spectrosc. 175 (2017) 76–91, https://doi.org/10.1016/j.saa.2016.12.005.
[30] M.J. Frisch, G.W. Trucks, H.B. Schlegel, G.E. Scuseria, M.A. Robb, J.R. Cheeseman, G. Scalmani, V. Barone, B. Mennucci, G.A. Petersson, H. Nakatsuji, M. Caricato, X. Li, H.P. Hratchian, A.F. Izmaylov, J. Bloino, G. Zheng, J.L. Sonnenberg, M. Hada, M. Ehara, K. Toyota, R. Fukuda, J. Hasegawa, M. Ishida, T. Nakajima, Y. Honda, O. Kitao, H. Nakai, T. Vreven, J.A. Montgomery Jr., J.E. Peralta, F. Ogliaro, M. Bearpark, J.J. Heyd, E. Brothers, K.N. Kudin, V.N. Staroverov, R. Kobayashi, J. Normand, K. Raghavachari, A. Rendell, J.C. Burant, S.S. Iyengar, J. Tomasi, M. Cossi, N. Rega, J.M. Millam, M. Klene, J.E. Knox, J.B. Cross, V. Bakken, C. Adamo, J. Jaramillo, R. Gomperts, R.E. Stratmann, O. Yazyev, A.J. Austin, R. Cammi, C. Pomelli, J.W. Ochterski, R.L. Martin, K. Morokuma, V.G. Zakrzewski, G.A. Voth, P. Salvador, J.J. Dannenberg, S. Dapprich, A.D. Daniels, O. Farkas, J.B. Foresman, J.V. Ortiz, J. Cioslowski, D.J. Fox, Gaussian 09, Revision A.02, Gaussian, Inc., Wallingford CT, 2009.
[31] http://cccbdb.nist.gov/vibscalejust.asp.
[32] P. Govindasamy, S. Gunasekaran, Quantum mechanical calculations and spectroscopic (FT-IR, FT-Raman and UV) investigations, molecular orbital, NLO, NBO, NLMO and MESP analysis of 4-[5-(4-methylphenyl)-3-(trifluoromethyl)-1H-pyrazol-1-yl] benzene-1-sulfonamide, J. Mol. Struct. 1081 (2015) 96–109, https://doi.org/10.1016/j.molstruc.2014.10.011.
[33] Rubarani P. Gangadharan, S. Sampath Krishnan, Natural bond orbital (NBO) population analysis of 1-azanapthalene-8-ol, Acta Phys. Pol. A 125 (1) (2014) 18–22, https://doi.org/10.12693/APhysPolA.125.18.
[34] Ira N. Levine, Quantum Chemistry - Textbook, Seventh Edition, Pearson Education, Inc, New York, 2014 (ISBN-13: 978-0-321-80345-0, Chapter 1).

[35] L.E.O.N.A.T. Lucia, S.B.Â.R.C.E.A. Gabriela, B.R.Â.N.Z.O.I. Ioan Viorel, Cyclic voltammetry for energy levels estimation of organic materials, U.P.B. Sci. Bull., Series B 75 (3) (2013) 111–118 (ISSN 1454-2331).
[36] J.L. Bredas, R. Silbey, D.S. Boudreux, R.R. Chance, Chain-length dependence of electronic and electrochemical properties of conjugated systems: polyacetylene, polyphenylene, polythiophene, and polypyrrole, J. Am. Chem. Soc. 105 (1983) 6555–6564, https://doi.org/10.1021/ja00360a004.
[37] Changqing Ye, Mingzhu Li, Jia Luo, Linfeng Chen, Zhengming Tang, Jian Pei, Lei Jiang, Yanlin Song, Daoben Zhu, Photo-induced amplification of readout contrast in nanoscale data storage, J. Mater. Chem. 22 (2012) 4299–4305, https://doi.org/10.1039/C2JM14923K.
[38] Anton Airinei, Nicusor Fifere, Mihaela Homocianu, Constantin Gaina, Viorica Gaina, Bogdan C. Simionescu, Optical properties of some new azo photoisomerizable bismaleimide derivatives, Int. J. Mol. Sci. 12 (2011) 6176–6193, https://doi.org/10.3390/ijms12096176.
[39] Ian Fleming, Molecular Orbitals and Organic Chemical Reactions. Chapter, 1, 2, 6, 8, John Wiley & Sons Inc. Reference Edition, 2010 (ISBN 978-0-470-74660-8).